Talanta 133 (2015) 45–51

Contents lists available at ScienceDirect

Talanta

journal homepage: www.elsevier.com/locate/talanta

Sequential injection technique as a tool for the automatic synthesis of silver nanoparticles in a greener way

Marieta L.C. Passos, Diana Costa, José L.F.C. Lima, M. Lúcia M.F.S. Saraiva *

REQUIMTE, Departamento de Ciências Químicas, Faculdade de Farmácia, Universidade do Porto, Rua de Jorge Viterbo Ferreira, 228, 4050-313 Porto, Portugal

ARTICLE INFO

Article history:
Received 31 October 2013
Received in revised form
28 January 2014
Accepted 21 April 2014
Available online 5 July 2014

Keywords:
Silver nanoparticles
Nanostructures
Green synthesis
Automation
Sequential injection analysis

ABSTRACT

This paper presents a new way to the synthesis of uniform and size-controlled silver nanoparticles by means of microreaction technology. It complies with the philosophy of green chemistry by developing a process that prevents pollution at source—by automation of the manipulations using microtubes manifolds and with the use of benign reagents and photochemistry to enhance the reaction of synthesis of Ag nanoparticles. Effect of hydrodynamic parameters (reagent volumes and volume flow rate) and concentrations (reducer and stabilizer), temperature, pH and UV irradiation time on morphology and size of nanoparticles was studied. The silver nanoparticles has been characterized by transmission electronic microscopy (TEM), electron diffraction X-ray spectroscopy (EDS), UV–vis spectra analysis, dynamic light scattering (DLS) and zeta potential measurements. Particles are mostly spherical in shape and have average sizes between 7 and 20 nm. The particle size can be controlled by changing not only the flow rate and UV light time exposition but also the reducer/$AgNO_3$ concentration ratio.

This is a sustainable and cost-saving methodology that guarantees not only reproducible synthesis, but also the changing of NPs characteristics at time by simple control of the fluid transport.

1. Introduction

Silver nanoparticles (AgNPs) use is widespread in diverse areas, including textile engineering, biotechnology, medicine, bioengineering, catalysis, water treatment, optics, electronics and also in food science [1]. The control of their physicochemical properties, namely its size and specific surface area, is a key parameter to determine their application. So, different methods have been reported for the synthesis of silver nanoparticles [2] namely by electrochemistry [3–5], thermal decomposition [6], laser ablation [7], microwave irradiation [8] and sonochemistry [9]. Chemical reduction, however, is the most frequently applied method since stable colloidal dispersions can be obtained [10,11]. The various species of Ag(I) are reduced originating silver atoms (Ag(0)) that then agglomerate into oligomeric clusters. These clusters eventually lead to the formation of colloidal Ag particles [1,11,12]. However, typical redox synthesis methods use, most of the times, hazardous chemicals as reducing agents [13]. So alternatives with the focus in using benign reagents have been growing, not only, regarding the reducing reagents [13] but also the NPs stabilizers [11,14]. However, many green reducer routes are very slow at room temperature so consequently need long periods of time to be complete [13]. Photoreduction can be an alternative. Harada et al. [15] made the photoreduction of Ag^+-containing water-in-[BMIm][BF_4] or water-in-[OMIm][BF_4] microemulsions in the presence of the non-ionic surfactant Tween 20 under high-pressure conditions of CO_2 [15]. The surfactant presence in the water-in-ionic liquid microemulsions promotes the stabilization of AgNPs and consequently the suppression of their growth and aggregation. Zhou et al. [16] prepared nanosilver/gelatine/CM-chitosan hydrogels by radiation crosslinking and reduction simultaneously. The formation of nanoparticles and nanorods was also described by Szymanska-Chargot et al. [17] being $AgNO_3$ in ethanol solution under UV light irradiation.

One of the goals of the present work is then to contribute to the developing of clean, environmental and human benign synthesis, aiming the use of nontoxic chemicals and photochemistry.

However, it is also extremely important to design a synthesis methodology that guarantees control of the experimental conditions as they determine the size, morphology, stability and chemical–physical properties of the AgNPs and consequently their application interest. For that a flow reactor device was used as advantages as scale- out, mass and heat rapid transportation and control, flexibility in space and time kinetic control are achieved [18–21].

The small size of the reaction channel, together with favourable heat and mass transport, allows for precise control of reaction and

* Corresponding author. Tel.: +351 220428679; fax: +351 226093483.
E-mail addresses: marietapassos@gmail.com (M.L.C. Passos), micf11178@ff.up.pt (D. Costa), limajlfc@ff.up.pt (J.L.F.C. Lima), lsaraiva@ff.up.pt (M.L.M.F.S. Saraiva).

http://dx.doi.org/10.1016/j.talanta.2014.04.089
0039-9140/

control of particle size, shape and composition, which is not easy to achieve in batch synthesis.

It is also achieved an enhanced efficiency of the UV light irradiation due to the extensive light penetration through the narrow channel compared to batch chamber reactors where the light penetration is not so effective due to the dilutions or the type of vessels used.

Continuous flow synthesis have been tested. However some disadvantages are noticed, namely partial mixing of reagents in batch mode [22–24], use of high temperatures [22,23,25], complex systems with microwaves oven [22,25] or ultrasonic stirring [25], high volumes of reagents [25] or a ineffective control of reagent volumes [24]. Additionally, this kind of systems do not present flexibility for changing volumes or reaction times as they present fixed configurations only physically changeable. Other flow techniques based in the sequential injection flow modes [26] (SIA) can, however, be used contributing to the design of more versatile modules. Its way of functioning is based in a computer-controlled nature that allows modifying the most relevant analytical parameters at run-time. It allows a great operational flexibility and the establishment of distinct strategies without physical reconfiguration. Moreover the bi-directional nature of fluid handling, the robustness, the ease of operation and the low reagent consumption inherent to SIA guarantee a great potential for its application in the silver nanoparticles synthesis. The incorporation of a photo reactor in a SIA module is also advantageous since the system can control precisely the irradiation time that leads to a great reproducibility of synthesis process and consequently of synthesized silver nanoparticles.

So, the objectives of this work were to develop an automatic module, based on sequential injection technique to synthesize silver nanoparticles, using at the same time green reducers and UV light for the reduction process. In addition to the synthesis, the present study was designed to characterize silver nanoparticles and to investigate the effect of different reducers, reagent concentrations, times of UV irradiation and other important parameters in this synthesis.

To the best of our knowledge this is the first report of a rapid, green and automatic protocol for size controlled silver nanoparticles synthesis, based on the sequential injection technique with a photoreactor and green reducers.

2. Experimental section

2.1. Reagents and solutions

All solutions were prepared with analytical reagent grade, high purity water (milli Q) with a specific conductivity $< 0.1\ \mu S\ cm^{-1}$.

A 5.00×10^{-3} mol L^{-1} silver nitrate (Merck) and a 0.10 mol L^{-1} tri-sodium citrate (Sigma) solutions were prepared from dissolution in water of appropriate amounts of the commercial powders.

The reducers used were ascorbic acid (Merck), glucose (Sigma) and glycerol (Sigma) in working standard solutions with concentrations between 2.50×10^{-5} and 2.00×10^{-2} mol L^{-1}. It was also used working standard solutions of NADH (Sigma) between 2.50×10^{-5} and 1.00×10^{-3} mol L^{-1} and of uric acid (Sigma) between 2.50×10^{-5} and 1.25×10^{-4} mol L^{-1}. All of these working standard solutions were prepared in water by dilution of the aqueous stock solutions prepared by dissolution of the appropriate amount of commercial powder or by dilution of the commercial solution in case of glycerol.

The carrier solution was 1.0×10^{-3} mol L^{-1} NaOH in water.

2.2. Automatic silver nanoparticles synthesis

2.2.1. Apparatus

The automatic SIA system (Fig. 1) consisted of a Gilson Minipuls 3 (VilliersleBel, France) peristaltic pump, equipped with a 1.30 mm

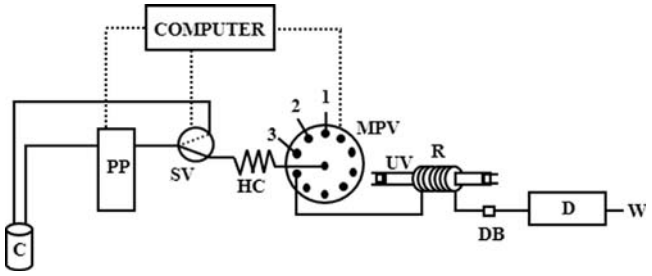

Fig. 1. SIA manifold for the silver nanoparticles synthesis. C, carrier; PP, peristaltic pump; SV, solenoid valve; HC, holding coil (2 m length/0.8 mm i. d.); MPV, multiposition selection valve; 1, $AgNO_3$ 5.00×10^{-3} mol L^{-1}; 2, tri-sodium citrate 0.10 mol mL^{-1}; 3, reducer; R, reaction coil (1 m, around the ultra-violet lamp); DB, de-bubbler; UV, ultra-violet lamp; D, spectrophotometric detector; W, waste.

i.d. Gilson PVC pumping tube and a 10-port selection valve (Valco, Vici C25-3180EMH, Houston, USA).

In order to guarantee reproducibility in the aspirated and propelled volumes, especially when dealing with reduced volumes, the starting position of the peristaltic pump at the beginning of each cycle was controlled. For that an NResearch 161 T031 solenoid valve (W. Caldwell, NJ, USA) (SV, Fig. 1) and a device placed on the peristaltic pump head were also introduced in the system [27].

Irradiation of the solutions with UV light was performed using a 15 W Philips TUV 15 W/G15T8 low pressure mercury lamp at 253.7 nm. The photochemical reactor was implemented by coiling a PTFE tubing (1 m and 0.8 mm i.d.) around the lamp, which was subsequently placed inside a protecting chamber.

As detection system, a Jenway (Model 6300, United Kingdom) spectrophotometric detector equipped with a flow-through cell of 30 μL was used. In the system, before the detector, it was placed a de-bubbler 006BT from Omnifit (Cambridge, England), to avoid that any bubble, formed in the reactor, could reach the detector.

All connections and the holding coil (HC, Fig. 1) that was serpentine-shaped in configuration were made with 0.8 mm i.d. PTFE tubing. This system was controlled by a homemade program written in QuickBasic language and implemented in a microcomputer equipped with an interface card (Advantech Corp., PCL 711B, San Jose, CA).

2.2.2. Automatic procedure

The developed analytical cycle (Table 1) began with the aspiration of 20 μL of $AgNO_3$ to the holding coil, followed by 20 μL of tri-sodium citrate and 20 μL of reducer solutions (steps 1–3). This aspirated sequence was sent by flow reversal, to the reaction coil (R, Fig. 1) placed around the UV lamp (UV, Fig. 1), through the port 4 (step 4). In the reaction coil the flow was stopped for 30 s (step 5), and thereafter, the fluids were sent to the detector (step 6) at 1 mL min^{-1} and a signal was recorded giving an indication about the yield of the synthesis, measuring the absorption signals in a fixed wavelength of 435 nm. After the detection the fluids resulted from each synthesis were collected for the Ag NPs characterization.

2.3. Characterization of AgNPs

2.3.1. UV–vis spectra analysis

The characterization of AgNPs could be done by UV–vis spectra analysis since their optical properties differ from those of bulk metal AgNPs. This NPs when dispersed in liquid media, display intense colors exhibiting a strong UV–vis absorption band attributed to surface plasmon resonance absorption. Surface plasmon resonance is a collective excitation of the electron in the conduction band near the surface of the nanoparticles [1,2,28]. Electrons are limited to specific vibrations modes by the particle's size

Table 1
SIA analytical cycle used in the silver nanoparticles automatic synthesis.

Step	Position	Volume (μL)	Time (s)	Flow rate (mL min^{-1})	Direction	Event
1	1	20	1.2	1	Aspiration	$AgNO_3$
2	2	20	1.2	1	Aspiration	Tri-sodium citrate
3	3	20	1.2	1	Aspiration	Reducer
4	4	500	30	1	Propulsion	Propulsion to the reaction coil
5	4	–	30	0	Stopped	Stopped flow in the reaction coil
6	4	2500	150	1	Propulsion	Propulsion to the detector

and shape [2]. Other factors as reaction stoichiometry, dielectric constants of both the metal and the surrounding medium, also affect the surface plasmon resonance absorption [1,29].

In this work, the UV–vis spectroscopic analysis of the AgNPs samples, collected at the end of the manifold, was performed by continuous scanning from 380 to 700 nm, using a Jasco (Model V-660, Japan) spectrophotometer.

2.3.2. Transmission electron microscopy (TEM) and electron diffraction X-ray spectroscopy (EDS)

The morphology and size of nanoparticles were determined by transmission electron microscopy (TEM) analysis in a JEOL JEM 1400 TEM (Tokyo, Japan). Images were digitally recorded using a Gatan SC 1000 ORIUS CCD camera (Warrendale, PA, USA). The TEM was equipped with an EDS Microanalysis System (Oxford Instruments) to determine the elemental composition of the samples.

2.3.3. Dynamic light scattering (DLS)

Dynamic light scattering (DLS), also known as photon correlation spectroscopy, was used to perform the particle size analysis. For that it was used a particle size analyzer (Brookhaven Instruments, Holtsville, NY, USA). DLS data were analyzed at 20 °C and with a fixed light incidence angle of 90°. The mean hydrodynamic diameter (*Z*-average) was determined as a measure of the width of the particle size distribution. This parameter was obtained by calculating the average of six runs.

2.3.4. Zeta potential measurements

Zeta potential provides important information about the nanoparticles dispersion since the charge magnitude is an indication of the repulsion between particles. So, the zeta potential can be used to predict the long-term stability of the nanoparticles dispersion [14].

The zeta potential was determined by measurement of the electrophoretic mobility using a zeta potential analyzer (Brookhaven Instruments, Holtsville, NY, USA). Samples were analyzed at 20 °C. The zeta potential of the analyzed samples was obtained by calculating the average of six runs.

3. Results and discussion

An important goal of green chemistry is to reduce or to eliminate the use or generation of feedstocks, products, byproducts, solvents, reagents, etc. that are hazardous to human health or the environment [30]. On this way, in this work it was used different strategies in order to comply with these objectives. One of these strategies was the development of an automatic system for the silver nanoparticles synthesis. Automation of chemical procedures reduce reagent and solvent consumption and consequently, reduce waste generation and avoid the side effects of the methods [30]. It was chosen the sequential injection analysis technique (SIA) [26] to implement the silver nanoparticles synthesis. The use of a flow system based in SIA technique, compared with a flow injection analysis (FIA) system, and due to its different way of operation, promotes a reduction of volume of about ten times in the use of carrier solution and reagents [30]. Furthermore, SIA systems are also simpler and can be adapted to different methodologies without manifold modifications. So, it assured the implementation of different synthesis protocols just by changing the solutions and the computer sequence.

Aiming an environmental benign chemical reduction it was tested different “green reducers” during this work. NADH, glucose, ascorbic acid, uric acid and glycerol was chosen, since all of them are not prejudicial for environment and human health. Beyond that, it was also used UV light for the reagents irradiation a strategy that enhance the reduction, with even a lower amount of reducer compound, following the green chemistry principles.

The study was started by testing the effect of each reducer in the synthesis of AgNPs by monitoring the absorption signals obtained with different concentrations of $AgNO_3$ in the presence and in the absence of the reducer. Since the solutions were irradiated with UV light, a signal was obtained even in the absence of a reducer. However, the presence of a reducer promoted an increase in the sensitivity around 3.6 times, and also an extend of the linearity of $AgNO_3$ concentrations. This results opened a possibility of using this kind of systems for quantitative purposes namely for monitoring any of the reducers in different samples. Beyond the eventual use for the quantitative objectives, the spectrophotometric detector was also used to confirm the reproducibility between syntheses.

Since the synthesis depends on the use of $AgNO_3$, reducer and stabilizer solutions, studies were carried out to establish the dependence of synthesis on reagent volumes between 10 and 75 μL. An increase in the absorption signal, measured in the spectrophotometer used as detector in the manifold, was observed between 10 and 20 μL. For volumes higher than 20 μL, a saturation of the detector was observed. It was therefore decided to use an aliquot of 20 μL of each reagent for further studies. With small volumes it was achieved an efficient interdispersion of the reagents in the system. Then, it was evaluated the effect on the synthesis of the molar ratio between $AgNO_3$ and the reducers. So, it was studied $AgNO_3$: reducer molar ratio between 0.25 and 200, for reducers like ascorbic acid or glucose, between 5 and 200 for NADH and between 40 and 200 for uric acid. The short interval used for uric acid was chosen due to its low solubility. Similarly, for NADH the ratios interval was reduced to minimize the costs of the synthesis due to the amount of spent compound. This study was performed using a fixed $AgNO_3$ concentration of 5.0×10^{-3} mol L^{-1}, and it was verified the effect of the different ratios in the maximum absorption signal of the plasmon band. When it was used ascorbic acid as reducer, the signal increases with the increasing of ratios up to 5. For ratio between 5 and 200 the behavior is the opposite, with the decrease in the signal. As with ascorbic acid, the NADH and the uric acid promoted a decrease effect on the signal, when the ratios increased up to 200. However for glucose the inverse has happened, since the increasing of the ratios between 0.25 and 5, lead to a decrease of the signal and between 5 and 200 the signals increased. These results confirm that the choice of the reducing agent has a great influence on the

synthesis, since its reductive ability determines the kinetics of the AgNPs formation [31].

After checking that ratios between $AgNO_3$ and reducers had an important influence in the synthesis, it became necessary to know the effect of reagents concentration in this reaction. For that, the concentrations of $AgNO_3$ were varied between 5.00×10^{-3} and 4.00×10^{-2} mol L^{-1} and the reducers between 1.25×10^{-4} and 1.00×10^{-3} mol L^{-1}, keeping unchanged the ratio of 40. The obtained results for these two combinations of $AgNO_3$ and reducer (ascorbic acid, glucose and NADH) concentrations are shown in Table 2.

It was verified that a decrease in $AgNO_3$ and reducer concentrations lead to a decrease in the particle sizes (around 11, 15 and 4 times smaller, for ascorbic acid, glucose and NADH, respectively). This decrease was accompanied and confirmed by a blue wavelength shift (21, 27 and 31 nm, for ascorbic acid, glucose and NADH, respectively). At the same time, the obtained NPs with low concentrations were more stable, since zeta potentials were more negative.

Beyond the ratio between $AgNO_3$ and reducer, the concentration of stabilizer has, also, a relevant importance in the synthesis, since it is essential in the control of the NPs growth and in the tuning of their chemical and physical properties [31,32]. The stabilizing agent molecules prevent the silver-AgNP bond formation and agglomeration by covering the surface of nanoparticles [33]. The type of stabilizer and its concentration affect the size, the size distribution and the capacity for aggregation [33]. In this work it was selected the tri-sodium citrate as stabilizer, since it was used before, with success, in different methods [33–35]. Its effect in the AgNPs synthesis was studied. The synthesis was done in the presence and in the absence of tri-sodium citrate (0.1 mol L^{-1}). The results, referred in Table 3, showed that zeta potential is more negative (between 4 and 10 times), in the presence of tri-sodium citrate, which means that this agent promote the stabilization of AgNPs, avoiding aggregation phenomena. The same table shows that the particles size decrease in the presence of tri-sodium citrate for half the size or even for thirty times less.

In order to verify if this effect was not resulting merely from the stabilizer action but was also due to a reductive action of the tri-sodium citrate, a study was done where it was compared the absorption signals from different $AgNO_3$: reducer ratios with signals obtained when the reducer was replaced for tri-sodium citrate with the same concentrations. It was verified that the increasing of reducer concentration promote an increment in the absorption signal, while the increasing of tri-sodium citrate did not. These results confirmed that the tri-sodium citrate had a stabilizer effect in the synthesis. So, it was decided to use 1.00×10^{-1} mol L^{-1} tri-sodium citrate, as stabilizer, for the further studies.

Since the adjustment of pH values of the medium can influence the absorption at the plasmon wavelength of the nanoparticles [36] this value was also changed during the optimization. It was studied, as carrier solutions, the effect of water, 0.1 mol L^{-1} phosphate buffer with pH = 7 and NaOH solution with concentrations between 10^{-7} and 10^{-2} mol L^{-1}. For this study it was used a molar ratio $AgNO_3$: reducer of 0.5 (for glycerol, ascorbic acid and glucose) and of 40 (for glycerol, ascorbic acid, glucose, NADH and uric acid). Regarding phosphate buffer no absorption plasmon band was observed, however with NaOH as carrier solution, even at a concentration of 10^{-7} mol L^{-1}, a band was observed, proving NPs synthesis. So, for $AgNO_3$: reducer ratio of 0.5 to ratio 40, the absorption maximum was increased with the increment of concentrations between 1×10^{-7} and 1×10^{-3} mol L^{-1} NaOH (Fig. 2). From this value of concentration the absorption decrease and it was observed a red shift of this maximum and a band enlargement, that could means an increase of particle size and aggregates formation and, also, an increase of the polydispersity in nanoparticles size (Fig. 2).

The exception to this behavior is for $AgNO_3$: glycerol of 40 and for $AgNO_3$: glucose of 0.5, since with these conditions the highest absorption signal was obtained with a 1×10^{-2} mol L^{-1} NaOH solution. However in these situations the enlargement and the red shift were also observed. So, the NaOH 1×10^{-3} mol L^{-1} was selected for further studies.

The influence of temperature was not very significant, since after evaluating between room temperature to 37 °C, with the various reducers the plasmon absorption bands were almost the same, except for the glucose with enhanced signals for 37 °C. So, the room temperature was chosen and used for further studies, since being favorable only for one reducer the use of a thermostatic water bath did not justify the increase of complexity of the manifold used for the NP synthesis.

Having optimized all of these parameters, the yield of the synthesis caused by the UV light in the SIA system was evaluated.

As it was referred before either the use of an automatic system (such as SIA) or a UV photoreactor are in agreement with some principles of the green chemistry, since they allow the reduction of reagent consumption and waste generation. Besides, their coupling

Table 2
$AgNO_3$ and reducer concentrations effect, keeping the ratio $AgNO_3$: reducer of 40.

	Ascorbic acid		Glucose		NADH	
$AgNO_3$ concentration (mol L^{-1})	**5.00×10^{-3}**	**4.00×10^{-2}**	**5.00×10^{-3}**	**4.00×10^{-2}**	**5.00×10^{-3}**	**4.00×10^{-2}**
Reducer concentration (mol L^{-1})	**1.25×10^{-4}**	**1.00×10^{-3}**	**1.25×10^{-4}**	**1.00×10^{-3}**	**1.25×10^{-4}**	**1.00×10^{-3}**
Particle size (nm)	7.02	76.24	6.01	92.79	178.04	769.77
Zeta potencial (mV)	−17.85	−12.28	−35.55	−10.72	−19.13	−9.47
Maximum wavelength (nm)	400	421	394	421	427	458

Table 3
Effect of presence or absence of tri-sodium citrate, in AgNPs synthesis.

Reducer	Reducer concentration (mol L^{-1})	$AgNO_3$:reducer ratio	Particle size (nm)		Zeta potential (mV)	
			No tri-sodium citrate	Tri-sodium citrate 0.10 mol L^{-1}	No tri-sodium citrate	Tri-sodium citrate 0.10 mol L^{-1}
NADH	2.50×10^{-4}	80	23.33	10.51	−7.86	−32.51
	1.00×10^{-3}	20	148.32	5.12	−5.33	−26.09
Ascorbicacid	2.50×10^{-4}	80	24.74	4.65	−6.07	−37.27
	1.00×10^{-3}	20	13.74	2.37	−3.84	−38.93

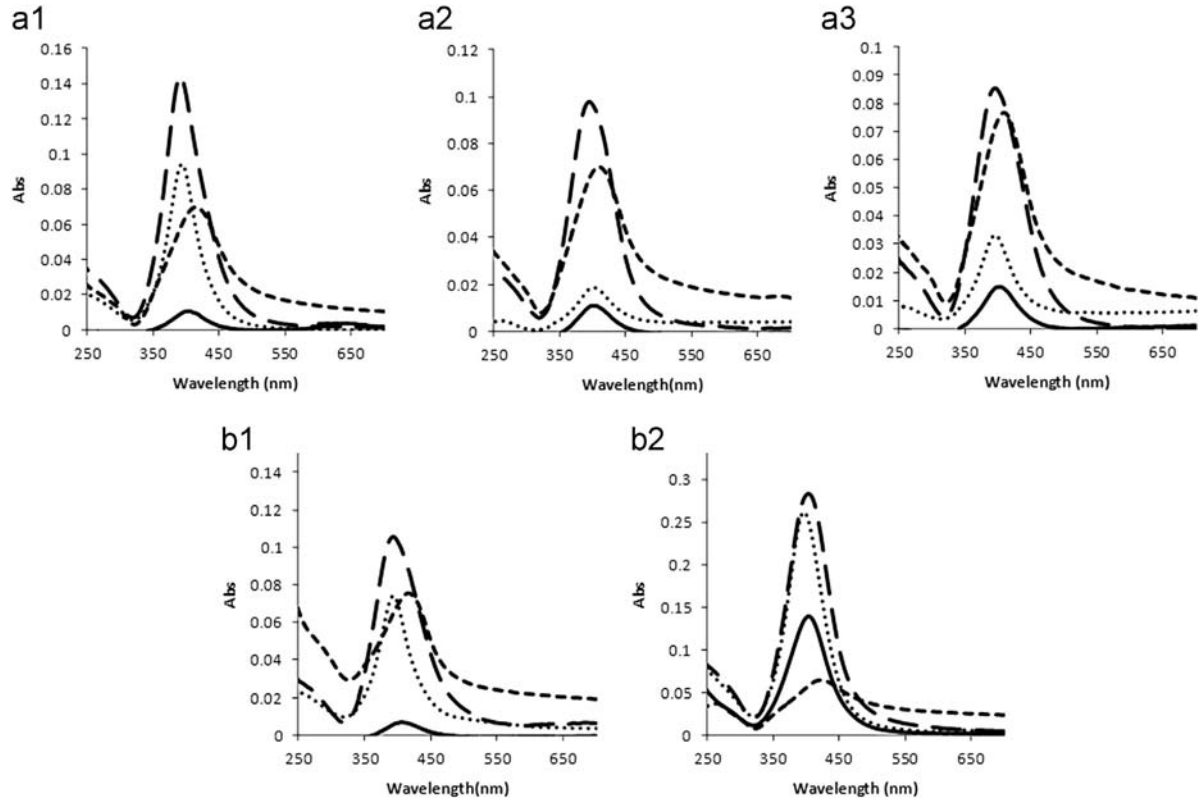

Fig. 2. NaOH concentration effect on the silver nanoparticles synthesis when it was used molar $AgNO_3$:reducer ratio of 40 (a1, a2, a3) and 0.5 (b1, b2). (a1, $AgNO_3$:ascorbic acid; a2, $AgNO_3$:glucose; a3, $AgNO_3$: uric acid), (b1, $AgNO_3$:glycerol; b2, $AgNO_3$:ascorbic acid). NaOH concentrations (mol L^{-1}): —— 0;····· 10^{-4}; — — 10^{-3}; - - - - 10^{-2}.

promotes a synthesis repeatability increment, since the use of an automatic system and consequently the absence of operator handling, allow a rigorous control of time irradiation.

In order to verify the UV light effect on the synthesis it was performed the synthesis with each chosen reducer, in the presence and in the absence of UV light.

A pronounced increase in the maximums of surface plasmon absorption bands were observed when the reagents were subjected to UV radiation. In fact with glucose as reducer, there was only when the reactor was irradiated that the band appear. For other reducers, the synthesis happen even without light but the surface plasmon absorption was increased about 27%, 283% and 343%, with the irradiation, for ascorbic acid, NADH and uric acid, respectively, in a $AgNO_3$:reducer ratio of 40.

After it was necessary to study the irradiation time over the reactor since it interfered directly in the irradiation time of the reagents and consequently the synthesis efficiency. It was adopted the stopped flow strategy in order to extend the reaction time under irradiation and avoid the increase of reagents dispersion by using longer reaction coils around the lamp. Different stopped flow periods were evaluated between 0 s (without stopped flow) and 90 s, for different reducers. This study was done using molar $AgNO_3$:reducer ratios of 0.5 and 40. It was verified, as it can be seen in Fig. 3 that for a $AgNO_3$:reducer ratio of 0.5 the higher signal was obtained with 30 s of stopped flow whereas for a ratio of 40 the best results were obtained with 60 s of stopped flow. For the following studies, it was chosen 30 s of irradiation time, as a compromise between spent time and synthesis efficiency.

Despite using a stopped flow in the reactor for the irradiation of the reagents, it was tested flow rates between 1 and 2 mL min^{-1}, for the propulsion of the fluids to and from the reactor. Results showed that a flow rate of 2 mL min^{-1} led to a decrease in the surface plasmon bands, probably due to a decrease in the reagents

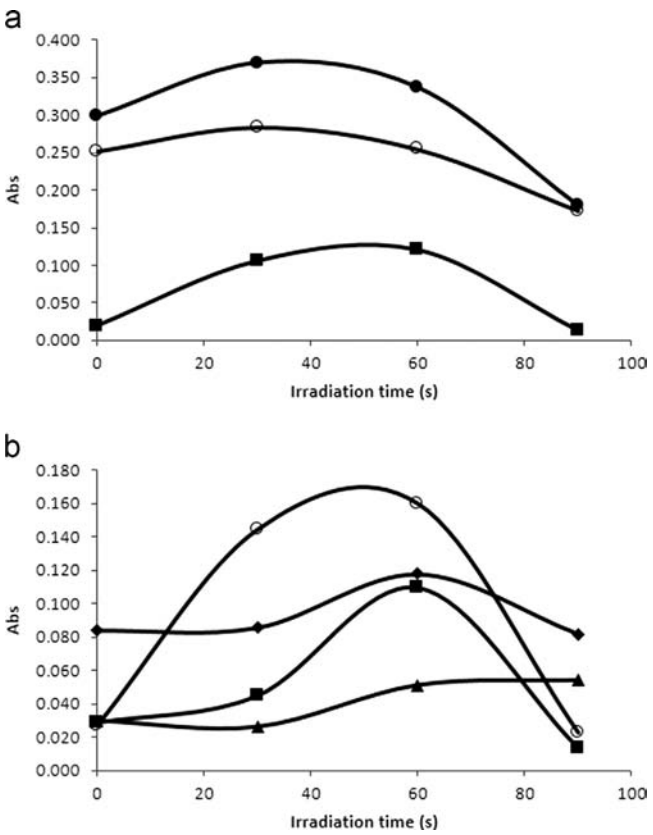

Fig. 3. Effect of irradiation time (stopped flow) on the silver nanoparticles synthesis when it was used molar $AgNO_3$: reducer ratio of 0.5 (a) and 40 (b). Reducer: glycerol (■), ascorbic acid (○), glucose (●), NADH (▲), uric acid (◆).

inter-dispersion. The flow rate of 1 mL min^{-1} was used as a compromise between synthesis efficiency and the time spent on each synthesis.

After the optimization of all these conditions silver nanoparticles were again synthesized using the different reducers in order to compare their effect in the synthesis with final conditions. It was verified that $AgNO_3$: reducer ratios had influence in the order of reducer effect. For a $AgNO_3$: reducer ratio of 40 ($AgNO_3$ 5.0×10^{-3} mol L^{-1} and reducer 1.25×10^{-4} mol L^{-1}), the increasing order of reducer effect in the synthesis is glucose, uric acid, NADH, glycerol and ascorbic acid. This order was obtained according to an increase of the plasmon band intensity. As with ratio of 40, for a ratio of 0.5 ($AgNO_3$ 5.0×10^{-3} mol L^{-1} and reducer 1.00×10^{-2} mol L^{-1}), the ascorbic acid shown a higher effect than glycerol. However, for this ratio, glucose had a higher effect than the ascorbic acid or glycerol. For this $AgNO_3$: reducer ratio, the increasing reducer effect is accompanied by an increase of the size of obtained nanoparticles (Table 4).

It was also verified that different reducers and different ratios between $AgNO_3$ and each reducer, led to different nanoparticles sizes (Table 4) and morphologies. Comparing the particles obtained with the two ratios of glycerol, it was verified that with lower concentration ($AgNO_3$: glycerol of 40) (Fig. 4a), the particles were bigger (around two times), more homogeneous in size and led to a higher absorption plasmon band than with ratio of 0.5 (Fig. 4b).

However, for glucose, this kind of behavior occurred for higher concentration (ratio of 0.5). For ascorbic acid with high concentration (ratio of 0.5) the produced nanoparticles were smaller (around 24%), led to a smaller (around 27% less) absorption plasmon band, and presented well defined borders. Using uric acid as reducer (ratio of 40), it was verified that nanoparticles were isolated (Fig. 5a) or organized in different branched structures (Fig. 5b).

With NADH as reducer (ratio of 40) the smallest nanoparticles with 4.6 nm (Table 4 and Fig. 6) could be seen.

The sizes obtained by TEM analysis were in general lower then by DLS. It happened since with DLS the measurement gives the hydrodynamic ray, which does not occur in TEM analysis.

The energy-dispersive spectroscopy (EDS) of the nanoparticles dispersion confirmed the presence of elemental silver signal and

Table 4
Sizes of silver nanoparticles obtained with two ratios of different reducers.

	$AgNO_3$: reducer ratio of 0.5		$AgNO_3$: reducer ratio of 40	
	TEM (nm)	DLS (nm)	TEM (nm)	DLS (nm)
Glycerol	5.6 ± 4.2	8.72 ± 1.27	12.7 ± 2.72	13.39 ± 1.53
Ascorbic acid	7.2 ± 2.4	10.88 ± 0.91	9.5 ± 2.8	7.02 ± 1.57
Glucose	10.1 ± 1.6	20.66 ± 0.11	6.2 ± 2.4	6.41 ± 1.41
NADH	–	–	4.6 ± 1.7	6.08 ± 1.31
Uric acid	–	–	9.3 ± 3.2	11.01 ± 1.99

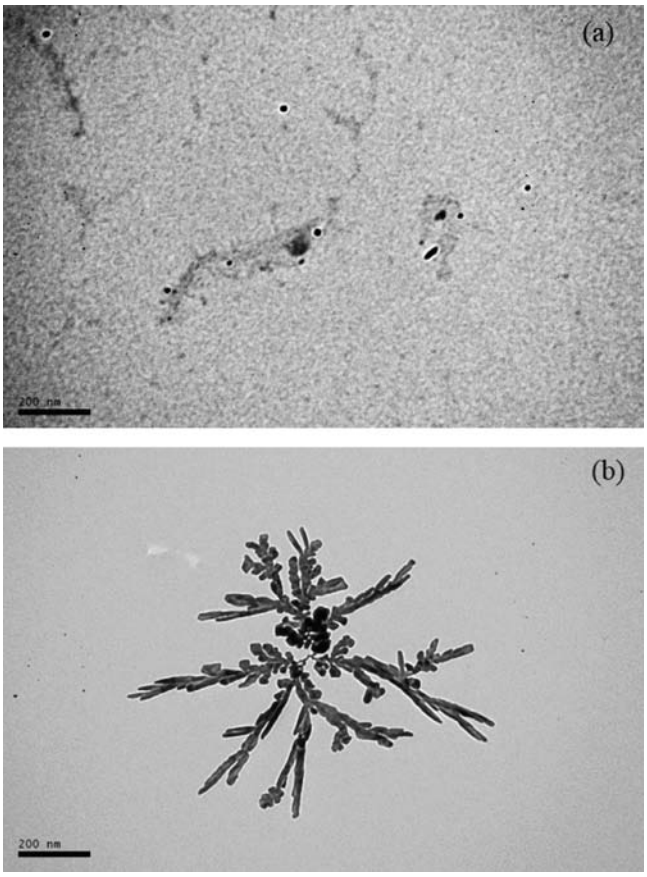

Fig. 5. Transmission electron microscopy (TEM) images of dispersed (a) and branched (b) silver nanoparticles synthesized using $AgNO_3$:uric acid ratio of 40 with an irradiation time of 30 s.

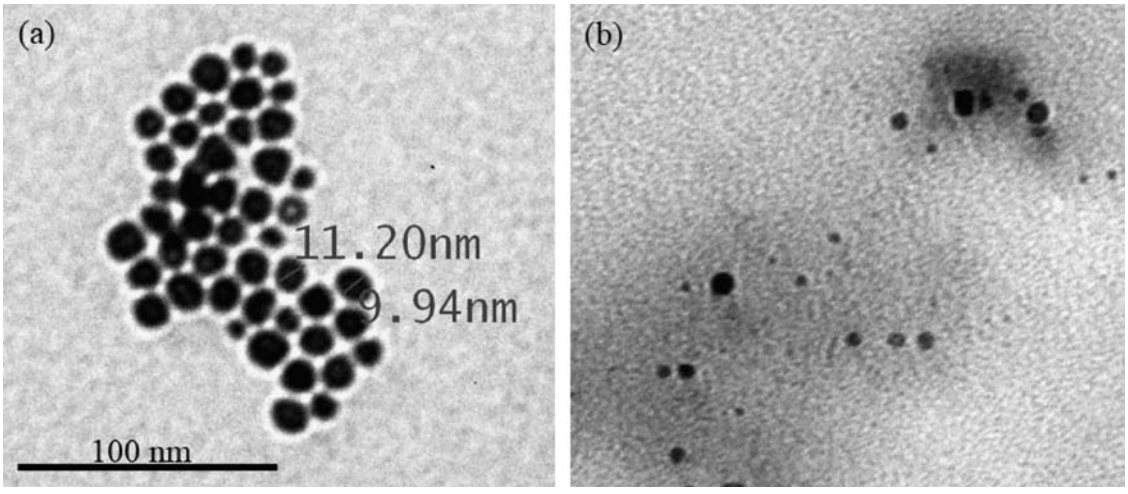

Fig. 4. Transmission electron microscopy (TEM) images of silver nanoparticles synthesized using a $AgNO_3$: glycerol ratio of 40 (a) and 0.5 (b).

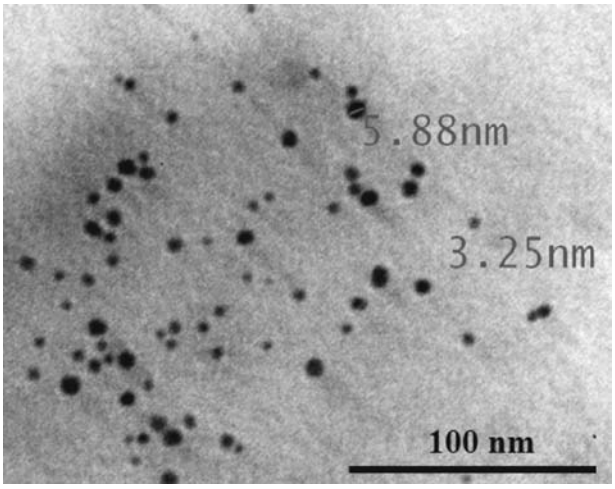

Fig. 6. Transmission electron microscopy (TEM) images of silver nanoparticles synthesized using $AgNO_3$:NADH ratio of 40 and an irradiation time of 30 s.

no peaks of other impurity were detected. The results indicate that the product is composed of high purity Ag nanoparticles. The absence of elemental nitrogen or elemental oxygen peaks prove that all silver nitrate was reduced to AgNPs.

Relative standard deviations (RSD%) between 1.1 and 5.0% were calculated based on the average sizes of particles. These particles were obtained in 10 different synthesis using each reducer, in an $AgNO_3$:reducer ratio of 0.5. Therefore, the methodology showed a good repeatability, confirming its applicability within synthesis of AgNPs using different reducers.

4. Conclusions

The automatic process developed for silver nanoparticles synthesis showed to be efficient, guaranteeing safer operation and environmental friendliness at reduced costs. A multi-step platform enables the fine tuning of NPs properties and the chemicals consume is lower even when compared with the other flow methods used to synthesize AgNPs. The proposed method only use around 5.2×10^{-6} mol of reagents in each synthesis, resulting in a waste generation of about 3 mL. However, the other reported flow methods for AgNPs synthesis use dozens or hundreds of mL of reagents due to a previous partial mixing of the reagents in batch mode [22–24] or an ineffective control of reagents volume since some were used as carrier and propelled in a continuous mode [24].

This module for NPs synthesis was implemented, for the first time and is very versatile, and flexible, since it allows at run time the changing of the synthesis protocols just by using the keyboard computer. Moreover different protocols can be performed independently or in sequence without stopping the flow. In addition it was observed an enhancement of the repeatability of the synthesis since the accuracy of reagent volumes and dispersion effects and the UV irradiation time, were performed without any operator interference. All of the reducers were also environment friendly and produced distinct NPs. UV light irradiation boosted the reducer's effect allowing a decrease in time and reagents and a greener methodology.

The effect of different reaction conditions was studied by UV–vis spectrophotometry, DLS, zeta potential, TEM and EDS measurements. Experimental results prove that $AgNO_3$: reducer ratio, reagent concentrations and volumes, the presence of a stabilizer and its concentration, pH, temperature, irradiation with UV light, conditioned the synthesis and consequently the size and shape of the silver nanoparticles obtained.

Acknowledgements

This work has been supported by Fundação para a Ciência e a Tecnologia through grant no. PEst-C/EQB/LA0006/2011. Marieta L.C. Passos thanks the Fundação para a Ciência e a Tecnologia, Pos-doc grant (SFRH/BPD/72378/2010) in the ambit of "POPH - QREN - Tipologia 4.1 - Formação Avançada" co-sponsored by FSE (European Social Fund) and national funds of MEC (Ministry of Education and Science).

References

[1] M. Ozyurek, N. Gungor, S. Baki, K. Guclu, R. Apak, Anal. Chem. 84 (2012) 8052–8059.
[2] M.G. Guzmán, J. Dille, S. Godet, World Acad. Sci., Eng. Technol. 19 (2008) 357–364.
[3] Z.Y. Tang, S.Q. Liu, S.J. Dong, E.K. Wang, J. Electroanal. Chem. 502 (2001) 146–151.
[4] M. Mazur, Electrochem. Commun. 6 (2004) 400–403.
[5] Z. Jian, Z. Xiang, W. Yongchang, Microelectron. Eng. 77 (2005) 58–62.
[6] Y.H. Kim, D.K. Lee, Y.S. Kang, Colloids Surf., A 257–258 (2005) 273–276.
[7] C.H. Bae, S.H. Nam, S.M. Park, Appl. Surf. Sci. 197 (2002) 628–634.
[8] K. Patel, S. Kapoor, D. Dave, T. Mukherjee, J. Chem. Sci. 117 (2005) 311–316.
[9] J.-p. Zhang, P. Chen, C.-h. Sun, X.-j. Hu, Appl. Catal., A 266 (2004) 49–54.
[10] A. Tao, P. Sinsermsuksakul, P. Yang, Angew. Chem. Int. Ed. 45 (2006) 4597–4601.
[11] M. Vijayakumar, K. Priya, F.T. Nancy, A. Noorlidah, A.B.A. Ahmed, Ind. Crops Prod. 41 (2013) 235–240.
[12] S. Kapoor, D. Lawless, P. Kennepohl, D. Meisel, N. Serpone, Langmuir 10 (1994) 3018–3022.
[13] S.K. Sivaraman, I. Elango, S. Kumar, V. Santhanam, Curr. Sci. 97 (2009) 1055–1059.
[14] A. Manivel, S. Anandan, Colloids Surf., A 395 (2012) 38–45.
[15] M. Harada, C. Kawasaki, K. Saijo, M. Demizu, Y. Kimura, J. Colloid Interface Sci. 343 (2010) 537–545.
[16] Y. Zhou, Y. Zhao, L. Wang, L. Xu, M. Zhai, S. Wei, Radiat. Phys. Chem. 81 (2012) 553–560.
[17] M. Szymanska-Chargot, A. Gruszecka, A. Smolira, K. Bederski, K. Gluch, J. Cytawa, L. Michalak, J. Alloys. Compd. 486 (2009) 66–69.
[18] A.M. Nightingale, J.H. Bannock, S.H. Krishnadasan, F.T.F. O'Mahony, S.A. Haque, J. Sloan, C. Drury, R. McIntyre, J.C. deMello, J. Mater. Chem. A 1 (2013) 4067–4076.
[19] S.A. Khan, S. Duraiswamy, Lab Chip 12 (2012) 1807–1812.
[20] Y. Song, J. Ding, Y. Wang, J. Phys. Chem. C 116 (2012) 11343–11350.
[21] Y. Song, S. Ji, Y.-J. Song, R. Li, J. Ding, X. Shen, R. Wang, R. Xu, X. Gu, J. Phys. Chem. C 117 (2013) 17274–17284.
[22] S. Horikoshi, H. Abe, K. Torigoe, M. Abe, N. Serpone, Nanoscale 2 (2010) 1441–1447.
[23] K.J. Hartlieb, M. Saunders, R.J.J. Jachuck, C.L. Raston, Green Chem. 12 (2010) 1012–1017.
[24] K. Herman, L. Szabo, L.F. Leopold, V. Chis, N. Leopold, Anal. Bioanal. Chem. 400 (2011) 815–820.
[25] G. Dzido, A.B. Jarzebski, J. Nanopart. Res. 13 (2011) 2533–2541.
[26] J. Ruzicka, G.D. Marshall, Anal. Chim. Acta 237 (1990) 329–343.
[27] M.L.C. Passos, M.L.M.F.S. Saraiva, J.L.F.C. Lima, M.G.A. Korn, J. Braz, Chem. Soc. 19 (2008) 563–568.
[28] V.K. Sharma, R.A. Yngard, Y. Lin, Adv. Colloid Interface Sci. 145 (2009) 83–96.
[29] S. Eustis, M.A. El-Sayed, Chem. Soc. Rev. 35 (2006) 209–217.
[30] L.H. Keith, L.U. Gron, J.L. Young, Chem. Rev. 107 (2007) 2695–2708.
[31] A.M. Signori, K.d.O. Santos, R. Eising, B.L. Albuquerque, F.C. Giacomelli, J.B. Domingos, Langmuir 26 (2010) 17772–17779.
[32] G.P. Li, Y.J. Luo, H.M. Tan, J. Solid State Chem. 178 (2005) 1038–1043.
[33] A. Sobczak-Kupiec, D. Malina, R. Kijkowska, Z. Wzorek, Micro Nano Lett. 7 (2012) 818–821.
[34] R. Patakfalvi, I. Dekany, J. Therm. Anal. Calorim. 79 (2005) 587–594.
[35] S.A. Cumberland, J.R. Lead, J. Chromatogr. A 1216 (2009) 9099–9105.
[36] C. Caro, P.M. Castillo, R. Klippstein, D. Pozo, A.P. Zaderenko, Silver nanoparticles: sensing and imaging applications, in: D.P. Perez (Ed.) Silver Nanoparticles, InTech, 2010, pp. 201-225.